REPORT DOCUMENTATION PAGE

Form Approved
OMB No. 0704-0188

1. AGENCY USE ONLY *(Leave Blank)*	2. REPORT DATE	3. REPORT TYPE AND DATES COVERED
	24 June 1999	10/98-9/99

4. TITLE AND SUBTITLE
Field Distribution in Thin Water Films – A Comparison of Theoretical and Empirical Trends

5. FUNDING NUMBERS
N00014-97-1-0417

Richard Carlin

6. AUTHOR(S)
D. L. Scovell, T. D. Pinkerton, V. K. Medvedev, and E. M. Stuve

7. PERFORMING ORGANIZATION NAME(S) AND ADDRESS(ES)
University of Washington
Department of Chemical Engineering
Box 351750
Seattle, WA 98195-1750

8. PERFORMING ORGANIZATION REPORT NUMBER
Technical Report No. 13

9. SPONSORING / MONITORING AGENCY NAME(S) AND ADDRESS(ES)
Office of Naval Research
800 N. Quincy Street
Arlington, VA 22217

11. SUPPLEMENTARY NOTES
Prepared for publication in the Proceedings of the International Symposium on New Directions in Electroanalytical Chemistry II, 1999 (Electrochemical Society Proceedings Volume)

12a. DISTRIBUTION / AVAILABILITY STATEMENT
This document has been approved for public release and sale; its distribution is unlimited.

12b. DISTRIBUTION CODE

13. ABSTRACT *(Maximum 200 words)*

Field ionization of thin water layers adsorbed onto a platinum field emitter tip was investigated by numerical simulation and analysis of experimental data. The numerical simulation, which includes a field-dependent relative permittivity, was developed to predict the field distribution around a water-covered field emitter tip. The model predicts that the dominant field occurs at the water-vacuum interface in thin layers. In the experiments, water adlayers were grown under field-free conditions by exposure of a cryogenically cooled emitter tip to water vapor in ultrahigh vacuum. Field ionization was probed by ramped field desorption (RFD) in which desorption of ionic species (hydrated protons) is measured while increasing the applied electric field linearly in time. The onset field of ionization decreased from 0.3 to 0.2 V/Å as temperature increased from 130 to 150 K. An activation barrier of 0.7 eV (16 kcal/mol) for ionization of water to produce hydrated protons and hydroxide ions was estimated from the temperature dependence of the onset field. The experimental trends agree with the predicted trends for thin water layers.

14. SUBJECT TERMS
Water, Field ionization, Platinum, Water ionization, Electric field effects, Dielectric properties

15. NUMBER OF PAGES
10

16. PRICE CODE

17. SECURITY CLASSIFICATION OF REPORT	18. SECURITY CLASSIFICATION OF THIS PAGE	19. SECURITY CLASSIFICATION OF ABSTRACT	20. LIMITATION OF ABSTRACT
Unclassified	Unclassified	Unclassified	

OFFICE OF NAVAL RESEARCH

Research Contract N00014-97-1-0417

Program Manager Richard Carlin

Technical Report No. 13

"Field Distributions in Thin Water Films – A Comparison of Theoretical and Experimental Trends"

by

D. L. Scovell, T. D. Pinkerton, V. K. Medvedev, and E. M. Stuve

Prepared for Publication

in

Proceedings of the International Symposium on New Directions in Electroanalytical Chemistry II, 1999 (Electrochemical Society Proceedings Volume)

University of Washington
Department of Chemical Engineering
Box 351750
Seattle, WA 98195-1750

June, 1999

FIELD DISTRIBUTIONS IN THIN WATER FILMS – A COMPARISON OF THEORETICAL AND EMPIRICAL TRENDS

Dawn L. Scovell, Tim D. Pinkerton, Valentin K. Medvedev, and Eric M. Stuve

University of Washington
Department of Chemical Engineering
Box 351750
Seattle, WA 98195-1750

ABSTRACT

Field ionization of thin water layers adsorbed onto a platinum field emitter was investigated by numerical simulation and analysis of experimental data. The numerical simulation, which includes a field-dependent relative permittivity, was developed to predict the field distribution around a water-covered field emitter tip. The model predicts that the dominant field occurs at the water-vacuum interface in thin layers. In the experiments, water adlayers were grown under field-free conditions by exposure of a cryogenically cooled emitter tip to water vapor in ultrahigh vacuum. Field ionization was probed by ramped field desorption (RFD) in which desorption of ionic species (hydrated protons) is measured while increasing the applied electric field linearly in time. The onset field of ionization decreased from 0.3 to 0.2 V/Å as temperature increased from 130 to 150 K. An activation barrier of 0.7 eV (16 kcal/mol) for ionization of water to produce hydrated protons and hydroxide ions was estimated from the temperature dependence of the onset field. The experimental trends agree with the predicted trends for thin water layers.

INTRODUCTION

High surface electric fields drive many important processes, such as electrochemistry, corrosion, and field emission. These surface fields, which are of the order of magnitude of 1 V/Å, are strong enough to make and break chemical bonds. The behavior of water in these fields is important because water is the primary component in electrochemical and corrosion processes as well as a major contaminant in the vacuum surrounding the field emitter arrays in flat panel displays. It is usually

Proceedings of the International Symposium on New Directions in Electroanalytical Chemistry II, 1999, Johna Leddy, Petr Vanysek, and Mark D. Porter (Eds.), The Electrochemical Society, Inc., 10 South Main Street, NJ 08534-2817, p. 6.

assumed that water amplifies the fields at electrode surfaces (1), but little is actually known about how water affects the electric field distribution.

Field emitters lend themselves to the study of the dielectric properties of water because they allow independent control of the electric field for fields as high as 5 V/Å. Multilayers of water can be vapor deposited by exposing a cryogenically cooled emitter tip to water vapor. The water deposited under these conditions is either amorphous ice, crystalline ice, or a mixture thereof. Under the appropriate conditions amorphous water-ice can undergo large translational movement, however, crystalline layers are stationary (2-4).

In this paper we report numerical and experimental results for the field ionization of water. Water was adsorbed at temperatures of 130 to 150 K onto a platinum field emitter tip under field-free conditions in ultrahigh vacuum. This temperature range was selected because the deposited water layer is crystalline and will be immobile during the course of the experiment. Ionization was examined by isothermal ramped field desorption (RFD) performed as a function of temperature and water layer thickness. We interpret the results in terms of the thickness dependence of the field at ionization onset and compare the experimental results to those of the numerical model (5).

NUMERICAL MODEL RESULTS

The applied field required to ionize a water layer increases with increasing thickness. This is easily explained by the dielectric screening of water; thicker water layers are more effective at screening the field at the water-vacuum interface. In the numerical simulation the water/tip system was modeled in spherical geometry. Key assumptions were that the tip is a perfect conductor and that no ions are present in the water layer (5). The potential distribution was found by numerically solving Poisson's equation for the water layer and Laplace's equation for the vacuum. The relative permittivity of the water was allowed to vary between low and high field limits of 80 and 2, respectively, with the transition occurring between 0.01 and 1 V/Å. The potentials in the water layer and vacuum were calculated as a function of tip potential and water thickness.

The model predicts that the field is always concentrated at the tip-water and water-vacuum interfaces. Fig. 1 shows the dependence of constant electric field lines on water thickness and applied electric field. The predominant field is predicted to be at the water-vacuum interface in thin water layers. As the water thickness increases, the field at the vacuum interface decreases and the field at the tip surface increases. When the water becomes sufficiently thick, the location of the predominant field shifts to the tip-water interface. The left-hand curve in Fig. 1 represents the locus of points where the field at the water-vacuum interface F_v is 0.4 V/Å while the right-hand curve represents the same for the field at the tip-water interface F_t. Ionization begins when either F_v or F_t becomes sufficiently large. As illustrated in Fig. 1, ionization is expected to begin at the vacuum interface in thin layers and at the tip surface in thick layers.

Positive ions formed at the vacuum interface will be ejected from the water layer when they are created, as shown in Fig. 2a. This implies that the onset of ionization is not influenced by the negative ions that are left in the adlayer. Positive ions formed at the tip surface, on the other hand, must migrate through the adlayer and then desorb from the surface before they can be detected, as shown in Fig. 2b. Thus, ions will be present in the water layer before they are detected in our measurements. A key assumption in the numerical model is that no ions are present in the adlayer. Clearly this is not true when ionization occurs at the tip surface and, as a result, the numerical model is not expected to accurately predict the onset of ionization in thick layers.

EQUIPMENT AND PROCEDURE

The experimental apparatus and procedure have been described previously (6) and will therefore be described only briefly. The vacuum chamber was pumped by a turbo-molecular pump and titanium getter pump to obtain a base pressure of 10^{-10} torr. A field emitter tip was used to generate electric fields as large as 4 V/Å. Ions produced by the tip were projected onto a pair of chevron microchannel plates (MCP) and directed onto a phosphor screen to form a greatly magnified, projection image of the tip surface. This image shows the detailed atomic arrangements of the hemispherical tip surface (7). Field ionization images were recorded with a CCD camera and VCR.

The tip was spot-welded to a 0.25 mm diameter heating loop mounted to the bottom of a cryogenically cooled downtube. The temperature was measured by a chromel/alumel thermocouple spot-welded to the heating loop. The desired temperature was maintained within ± 0.3 K by a PID temperature controller connected to a d.c. power supply for resistive heating. A high voltage feedthrough at the bottom of the downtube provided high voltage isolation for the heating loop/tip assembly.

The field emitter tip was electrochemically etched from 0.013 mm diameter platinum wire at 2-3 V d.c. in a molten mixture of sodium chloride and sodium nitrate. The tip radius was determined from the best imaging field of 3.75 V/Å for neon (8). The relationship between the applied potential V_t and the applied field F_{app} is

$$F_{app} = V_t / \beta r_t , \qquad [1]$$

where β is the shape factor and r_t is the tip radius. The shape factor is 5 for a typical emitter tip (9). The tip radius in these experiments ranged from 335 to 374 Å. Tip radii determined from the best imaging field were within 20% of those estimated by counting the number of lattice steps between the (001) and (113) planes in the field ionization images. The relative error in the electric fields reported in these experiments is less than 5%. In this paper the term "applied field" is used to describe the field that would occur for bare tip surface in vacuum for a given applied tip potential.

A three-step procedure was used to ensure that the tip was free from contaminants at the beginning of each experimental run. First, the tip was heated to 500 K to desorb any water from the tip and heating loop assembly. Second, any remaining contaminants were field desorbed from the tip by imaging in neon and hydrogen. Finally, a small amount of platinum was field desorbed in neon to ensure that the surface was atomically clean.

Prior to dosing, water was degassed with both liquid nitrogen and dry ice in several freeze-thaw cycles. Water was introduced into the background of the vacuum chamber through a variable leak valve to produce a uniform layer of ice on the tip under field-free conditions. The tip was held at the desired temperature during dosing. The tip was exposed to 5.0×10^{-7} torr of water for 2 to 60 minutes. Pressures of less than 5.0×10^{-9} torr were typically achieved within 2 to 10 minutes after dosing. The ice layer thickness was estimated from the molecular flux during dosing and adjusted for any desorption during chamber pump down. The sticking coefficient was assumed to be unity, and the ice density was varied linearly from 0.8 g/cm^3 at 80 K to 0.93 g/cm^3 at 130 K (10). Water thicknesses of 50 to 3600 Å were obtained.

Ramped field desorption (RFD) spectra were obtained after removing water from the background gas (11). During the RFD runs, the potential applied to the tip was increased at a constant rate. When the field becomes sufficiently large, ions are created, desorb from the water layer, radially accelerate away from the tip and are then detected when they arrived at the MCP/phosphor screen assembly. The signal from the phosphor screen was monitored by two rate meters, each with a time constant of 0.1 s. The first rate meter was always set to a sensitivity of 300 counts per second (CPS) full scale, while the second was adjusted to capture the entire peak. The first rate meter was used to determine ionization onset.

EXPERIMENTAL RESULTS

The effects of temperature and ice thickness on the ionization of water were studied. The ionization onset field $F_{app,o}$ defined experimentally as the applied field at which ionization reaches 10 counts/s, was measured as a function of the dimensionless ice thickness at temperatures between 130 and 150 K. The dimensionless thickness x is the ratio of the thickness of the ice layer to the tip radius. The ionization threshold of 10 counts/s is lower than used previously (6) because the background noise levels were lower in these experiments. The applied field was ramped at 6 mVÅ^{-1}s^{-1} for all runs. Fig. 3 shows that the dependence of the onset field at 133 K for thin layers of water is linear with thickness.

The slope $dF_{app,o}/dx$ is strongly dependent upon temperature. Fig. 4 shows the temperature dependence of $dF_{app,o}/dx$ for thin water adlayers. The open circles are the experimental data. The slope, $dF_{app,o}/dx$, ranges from 0.2-0.3 V / Å. The slopes and error bars were determined by linear regression. The solid line in Fig. 4 is the slope predicted by the numerical model.

Extrapolation of the data in Fig. 3 to zero thickness gives an estimate of the actual field needed for ionization, F_o. Extrapolation is necessary to correct for screening of the field by water layers of finite thickness. The onset field F_o is a true, rather than applied, field because the influence of water layer thickness has been removed. The extrapolated onset fields are shown in Fig. 5. The trend in the extrapolated onset field is linear between 130 and 150 K.

DISCUSSION

The numerical model predicts that ionization occurs at the vacuum interface in thin water layers. Fig. 1 shows that in the limit of zero thickness, the applied field is the same as the field at which water ionizes at the vacuum interface F_v. Thus, the vacuum field is the same as the onset field F_o. From Fig. 1, F_v is 0.31 V/Å at 133 K. Values for F_v as a function of temperature are shown in Fig. 5.

The solid line in Fig. 3 is the predicted trend for F_v = 0.31 V/Å. The predicted trend agrees well with the trend of the experimental data. The best way to evaluate the numerical model is to compare the predicted and measured values of $dF_{app,o}/dx$ because the value of the vacuum field (i.e., the y-intercept of Fig. 3) was determined from the experimental data. The temperature dependence of the predicted slope is the solid line in Fig. 4. The temperature dependence of the predicted slope is within the error of the experimentally obtained slopes.

The temperature dependence of the onset field of ionization provides information about the energetics of the ionization event. As discussed in a previous publication (6) the rate of thermally excited ionization may be written as:

$$r_{ion} = n_w \upsilon \exp\left[\frac{V_1 F_o + H_a - (\Delta P)F_o}{kT}\right], \qquad [2]$$

where n_w is the areal density of water, ν the pre-exponential factor, V_1 the field dependence of the potential of curve crossing between the neutral and ionic potential energy curves, F_o the onset field, H_a the field-free activation barrier, ΔP the difference between the dipole moment of the final and initial states, k Boltzmann's constant, and T temperature. This expression assumes that the neutral and ionic potential energy curves are straight in the region of crossing.

As a constant detection rate was used to determine the onset of ionization, an instrumental constant I_c can be estimated from Eqn. 2:

$$I_c = -\ln\left[\frac{r_{ion,o}}{n_w \upsilon}\right] = \frac{V_1 F_o + H_a - (\Delta P)F_o}{kT}, \qquad [3]$$

where $r_{ion,o}$ is derived from the specified detection rate of 10 counts/s and the hemispherical area of the tip. The quantity in square brackets in Eqn. 2 is assumed to be independent of field. The instrumental constant is 45 for the specified detection rate and a tip radius of 350 Å (6). Solving for F_o gives

$$F_o = \frac{1}{V_1 - (\Delta P)}(H_a - I_c kT). \qquad [4]$$

This expression predicts a linear relationship between the onset field for ionization and the temperature. As shown in Fig. 5 the RFD data are linear. The linear relationship is in excellent agreement with results reported by Stintz and Panitz (12).

Extrapolation of the data to zero field provides an estimate of the field free activation barrier. As shown in Fig. 5, the extrapolated temperature for crystalline ice is 216 K, which corresponds to a field-free activation barrier for ionization of 0.7 ± 0.1 eV. This compares well with results from d.c. conductivity experiments for water between platinum electrodes which show that 0.74 eV is required to form a pair of ions from two solvated water molecules (13). The error in the field-free activation energy is large because the data were taken over a relatively narrow temperature range and have large error bars. It may be possible to obtain a better estimate of the field-free activation energy for the crystalline phase by extending the temperature range. This can be done by depositing crystalline ice at temperatures above 145 K (14, 15) and performing the RFD experiment at lower temperatures.

The slope in Fig. 5 can be used to estimate the dipole moment of the layer. If V_1 is negligible (6) then the slope of –0.003614 $VÅ^{-1}K^{-1}$ is equivalent to a dipole moment of –5.1 Debye. If the final state hydronium ion is assumed to have a small dipole moment ($P_f \approx 0$), then this result gives a value of 5.1 Debye for the initial state water molecule. The dipole moment of liquid water has been calculated to be 2.4 – 3.0 Debye and that of hexagonal ice is predicted to be 3.1 Debye (16). A likely explanation for the differences between the experimental and calculated values is that V_1 is not zero. Unfortunately, the relative importance of the curve crossing (V_1) and the dipolar interaction effects (ΔP) cannot be measured with this method, and further research is necessary to devise a means for measuring these quantities independently.

CONCLUSIONS

The ionization of water layers adsorbed under field-free conditions depends upon the thickness of the water. Our numerical model predicts that thin water layers ionize at the vacuum interface. The trends measured in our ramped field desorption experiments are consistent with the model predictions for thin layers. The experimental data were used to estimate a field-free activation barrier of 0.7 eV, which agrees well with the value of 0.74 eV obtained by others. The experimental data was also used to estimate a dipole moment of the layer of 5.1 Debye.

ACKNOWLEDGMENTS

We gratefully acknowledge support of this work from the Office of Naval Research.

REFERENCES

1. D. M. Kolb and C. Franke, *Appl. Phys. A*, **49**, 379 (1989).
2. R. S. Smith and B. D. Kay, *Surf. Rev. Letters*, **4**, 781 (1997).
3. P. Jenniskens, S. F. Banham, D. F. Blake, and M. R. S. McCoustra, *J. Chem. Phys.*, **107**, 1232 (1997).
4. G. P. Johari, G. Fleissner, A. Hallbrucker, and E. Mayer, *J. Phys. Chem.*, **98**, 4719 (1994).
5. D. L. Scovell, T. D. Pinkerton, B. A. Finlayson, and E. M. Stuve, *Chem. Phys. Lett.*, **294**, 255 (1998).
6. T. D. Pinkerton, D. L. Scovell, A. L. Johnson, B. Xia, V. K. Medvedev, and E. M. Stuve, *Langmuir*, accepted (1999).
7. T. Sakurai, A. Sakai, and H. W. Pickering, *Atom-Probe Field Ion Microscopy and its Applications*, Academic Press, Inc., Boston, (1989).
8. T. T. Tsong, *Atom-Probe Field Ion Microscopy*, Cambridge University Press, Cambridge, (1990).
9. R. Gomer, *Field Emission and Field Ionization*, Harvard University Press, Cambridge, (1961).
10. D. E. Brown, S. M. George, C. Huang, E. K. L. Wong, K. B. Rider, R. S. Smith, and B. D. Kay, *J. Phys. Chem.*, **100**, 4988 (1996).
11. A. Stintz and J. A. Panitz, *J. Appl. Phys.*, **72**, 741 (1992).
12. A. Stintz and J. A. Panitz, *Surf. Sci.*, **296**, 75 (1993).
13. P. V. Hobbs, *Ice Physics*, Clarendon Press, Oxford, (1974).
14. R. S. Smith, C. Huang, E. K. L. Wong, and B. D. Kay, *Surf. Sci.*, **367**, L13 (1996).
15. N. Materer, U. Starke, A. Barbieri, M. A. V. Hove, G. A. Somorjai, G. J. Kroes, and C. Minot, *Surf. Sci.*, **381**, 190 (1997).
16. E. R. Batista, S. S. Xantheas, and H. Jonsson, *J. Chem. Phys.*, **109**, 4546 (1998).

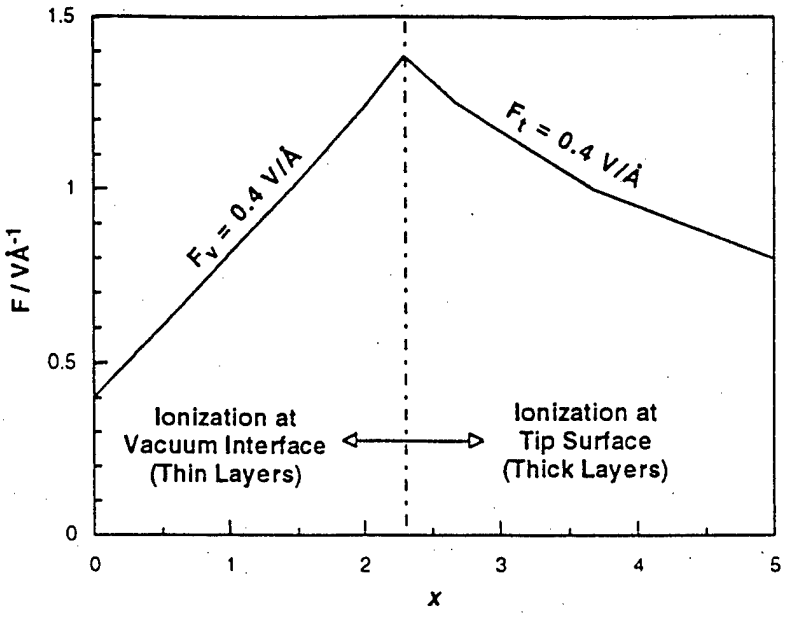

Fig. 1. Lines of constant vacuum field F_v and tip field F_t of 0.4 V/Å as a function of dimensionless thickness x. Dimensionless thickness is the ratio of the water thickness to the tip radius. The dashed line is the thickness at which the predominant field changes from the water-vacuum to the tip-water interface. In thin layers ionization is expected to occur at the vacuum interface and in thick layers it is expected to occur at the tip surface.

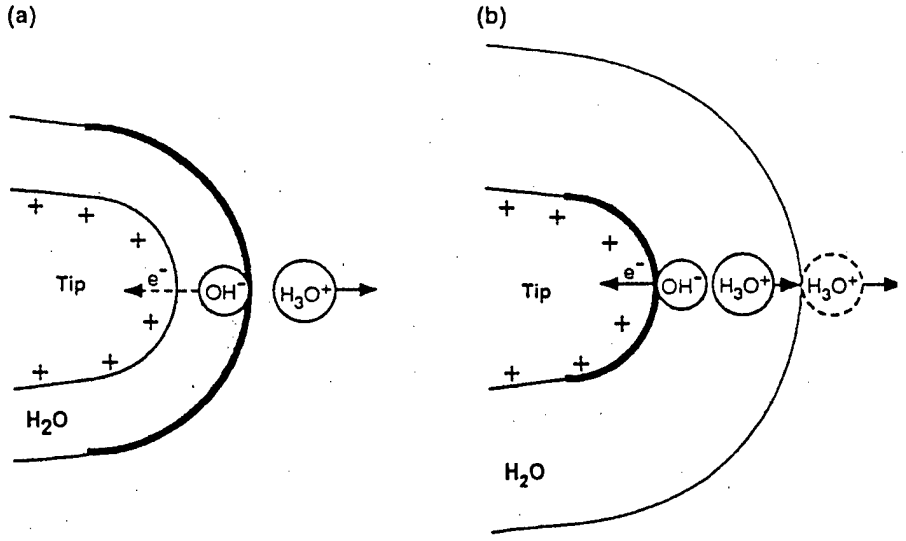

Fig. 2. Schematic of the ionization process at (a) the water-vacuum interface and (b) at the tip surface. The heavy lines represent the interface where ionization occurs.

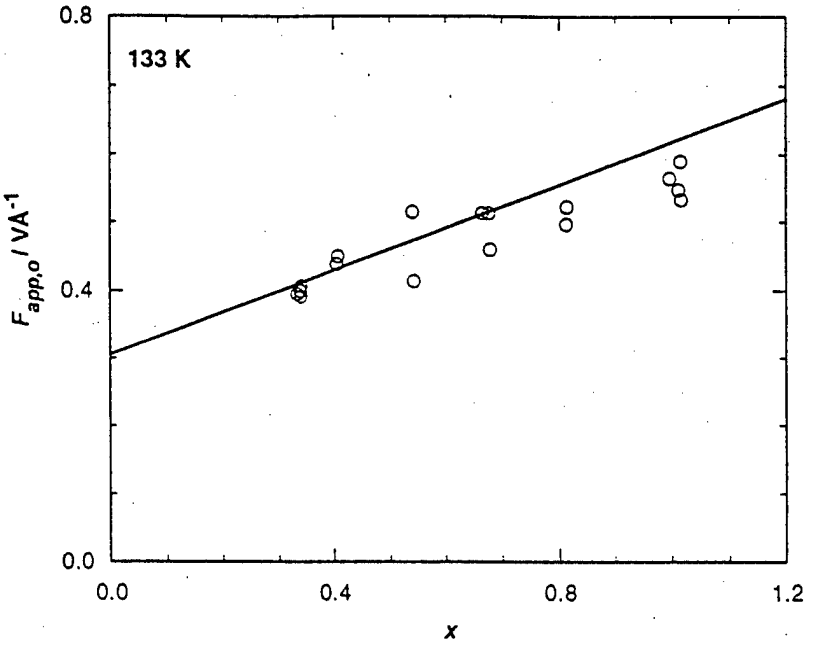

Fig. 3. Applied field at ionization onset as a function of deposited ice thickness x at 133 K. The solid line is the numerical prediction for a vacuum field F_v of 0.31 V/Å. The circles are the experimental data.

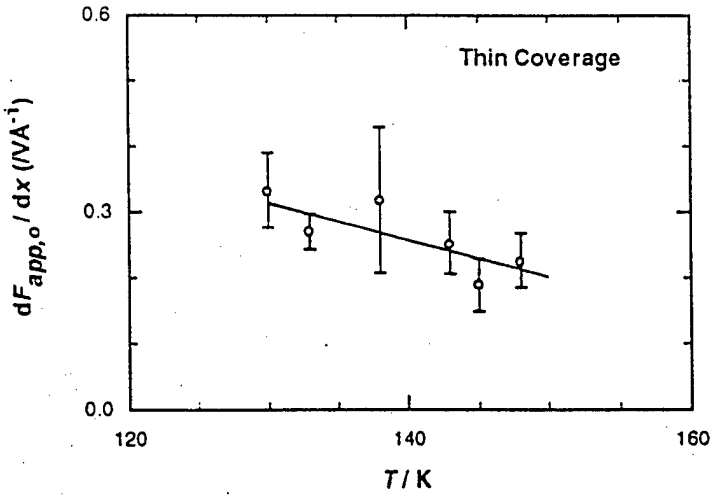

Fig. 4. Temperature dependence of the slope $dF_{app,o}/dx$ for thin coverages. The open circles are the measured data and the solid line is the numerical prediction.

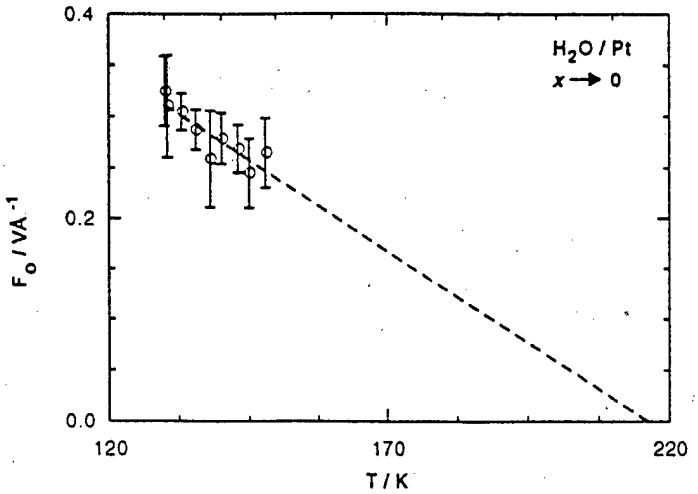

Fig. 5. The temperature dependence of the onset field F_o required to ionize thin layers of water. This field was determined by the y-intercept in plots of applied field $F_{app,o}$ vs. thickness x (e.g., Fig. 3). Note that in the numerical prediction F_o is equivalent to the field at the vacuum interface F_v.